catalysts

Supplementary Information

Eco-toxicological and kinetic evaluation of TiO_2 and ZnO nanophotocatalysts in degradation of organic dye

Sajjad Khezrianjoo [a,1], Jechan Lee [b,1], Ki-Hyun Kim [a,*], Vanish Kumar [c,*]

[a] Air Quality & Materials Application Lab, Department of Civil & Environmental Engineering, Hanyang University, 222 Wangsimni-Ro, Seoul 04763, Republic of Korea
[b] Department of Environmental and Safety Engineering, Ajou University, 206 Worldcup-ro, Suwon 16499, Republic of Korea
[c] National Agri-Food Biotechnology Institute (NABI), S.A.S. Nagar, Punjab, 140306, India
[1] These authors are co-first authors as they contributed equally.
* Correspondce Email: kkim61@hanyang.ac.kr; vanish.saini01@gmail.com

UV-Vis spectra analysis as well as image of germination and root growth of *L. sativum* L.

FB1 is a mono azo dye in which the strong absorbance in the visible region (570 nm) is related to the chromophore part of the molecular structure (azo linkage). Absorbance peaks for the naphthalene and benzene rings appeared in the UV region (about 300 nm) [1]. Full spectra scanning of the target dye was followed during the time-course of the HPO process while experiments were performed after a 1 h dark pre-adsorption period or without it (Figures S1 A, B, C and D). A gradual disappearance of the absorbance peaks around 570 nm observed during the time-course showed almost perfect degradation of the main chromophore. Therefore, nearly complete decolorization was achieved in the presence of TiO_2 or ZnO catalysts. It has been reported that the intensity of the azo band (visible light chromophore) decreases with time more rapidly than the chromophore of the aromatic ring [2]. The slower decrease of the previous chromophore could be due to the formation of aromatic byproducts before destruction of these byproducts [2].

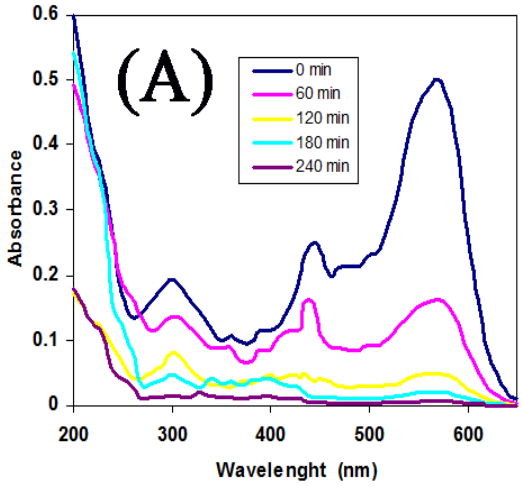

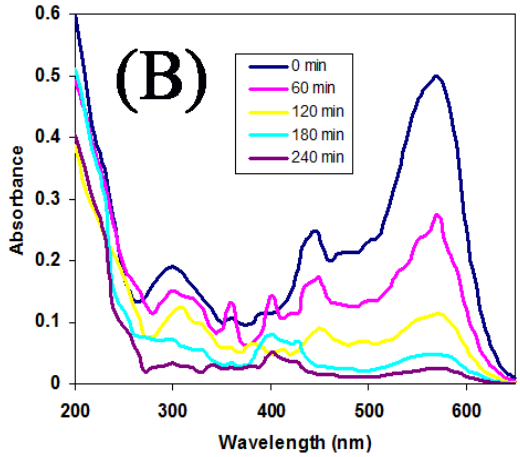

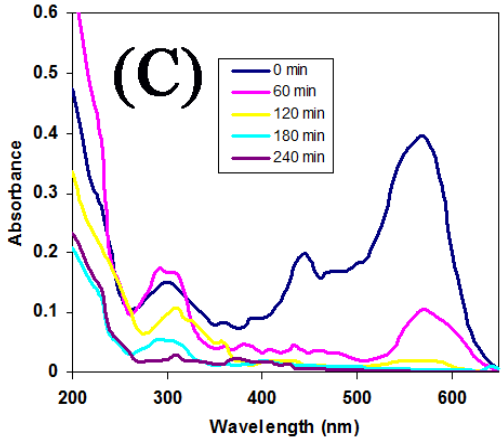

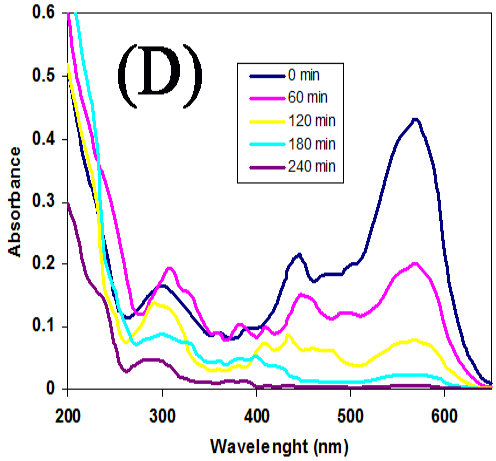

Figure S1. UV-Vis spectra changes of FB1 at different irradiation times; $[FB1]_0$ = 50 (mg/L), $[TiO_2]$ = 0.8 (g/L), [ZnO] = 1.2 (g/L), T = 25 °C and pH 6.7 (neutral). (A): UV-TiO_2 process without pre-adsorption period, (B): UV-ZnO process without pre-adsorption period, (C): UV-TiO_2 process with pre-adsorption period and (D): UV-ZnO process with pre-adsorption period.

An image of one sample of replicate plates used in the bioassay experiments is presented in Figure S2 (A to W). The effect of the pre-adsorption period on the detoxification process using both catalysts (TiO_2 and ZnO) has been analyzed by scanning the toxic properties of FB1 and its degradation byproducts. Consequently, the mean number of *L. sativum* L. germinated seeds (as well as its root length) were recorded during the degradation process to determine the germination index (*GI*%). Images A, B, C, D, E and F are related to the UV-TiO_2 process without a pre-adsorption period. Images A, G, H, I, J and K are related to the UV-ZnO process without a pre-adsorption period after 0, 60, 120, 180, 240 and 300 min of illumination, respectively. Images L, M, N, O, P and Q are related to the UV-TiO_2 process with a pre-adsorption period, and images R, S, T, U, V and W are related to the UV-ZnO process with pre-adsorption periods after 0, 60, 120, 180, 240 and 300 min of irradiation, respectively. Images L and R have been captured when the FB1 solution was circulated in the presence of TiO_2 or ZnO catalysts for 60 min while the UV light was absent (darkness). Therefore, 21% and 14% dye were adsorbed on TiO_2 or ZnO surfaces, respectively.

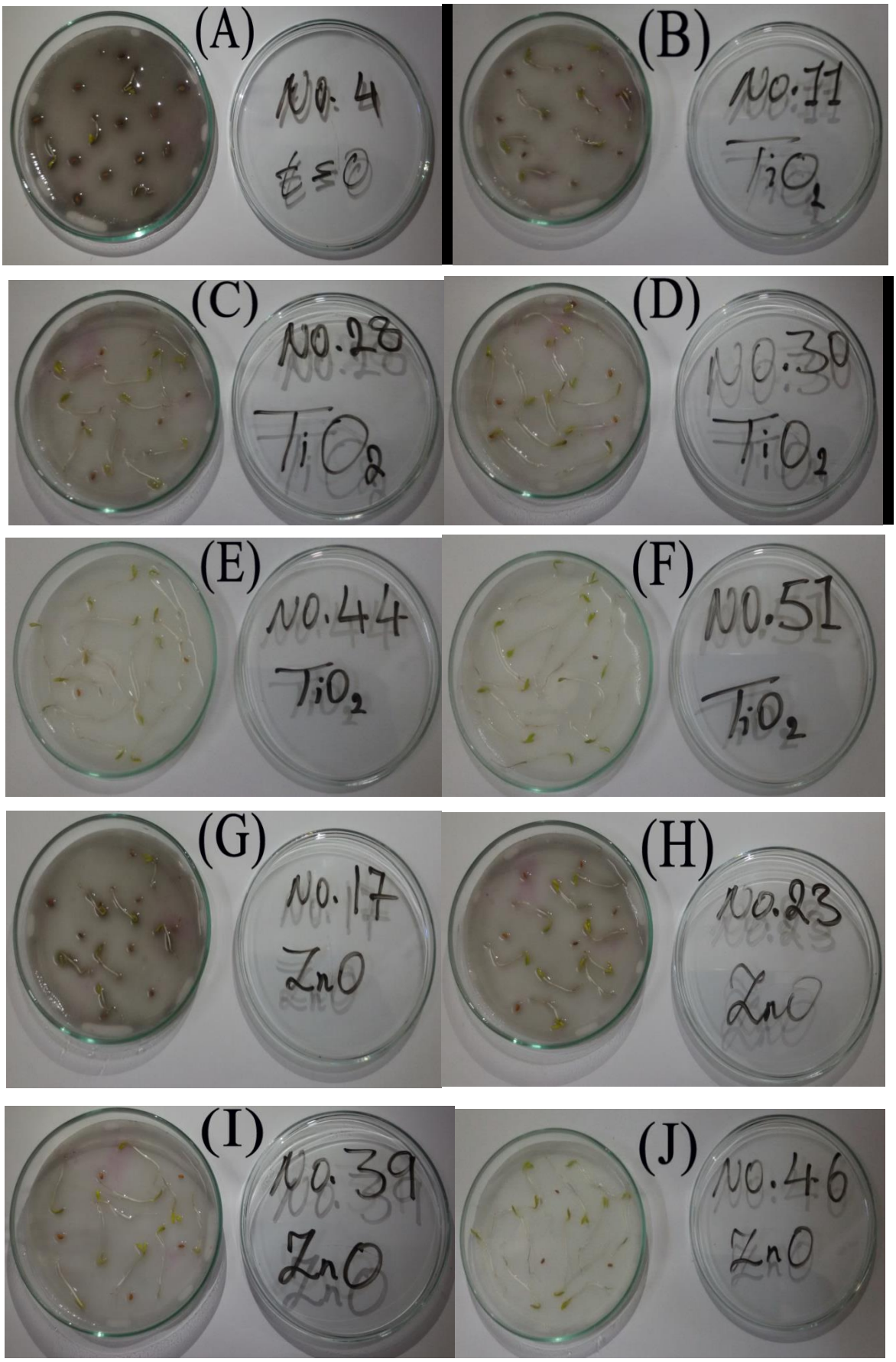
(A)
No. 4
(B)
No. 11
TiO2
(C)
No. 28
TiO2
(D)
No. 30
TiO2
(E)
No. 44
TiO2
(F)
No. 51
TiO2
(G)
No. 17
ZnO
(H)
No. 23
ZnO
(I)
No. 39
ZnO
(J)
No. 46
ZnO

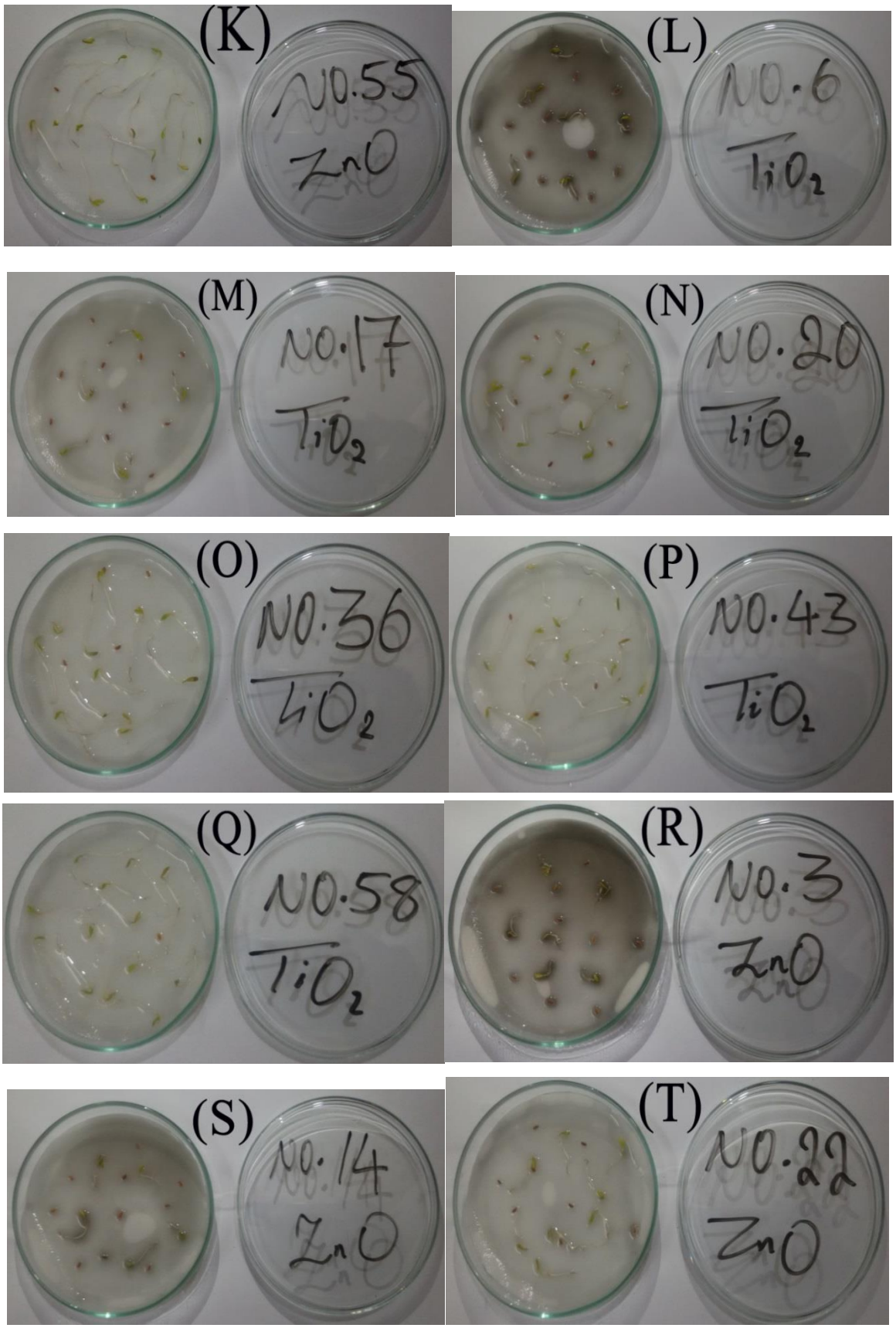
(K)
NO.55
ZnO
(L)
NO.6
TiO2
(M)
NO.17
TiO2
(N)
NO.20
TiO2
(O)
NO.36
TiO2
(P)
NO.43
TiO2
(Q)
NO.58
TiO2
(R)
NO.3
ZnO
(S)
NO.14
ZnO
(T)
NO.22
ZnO

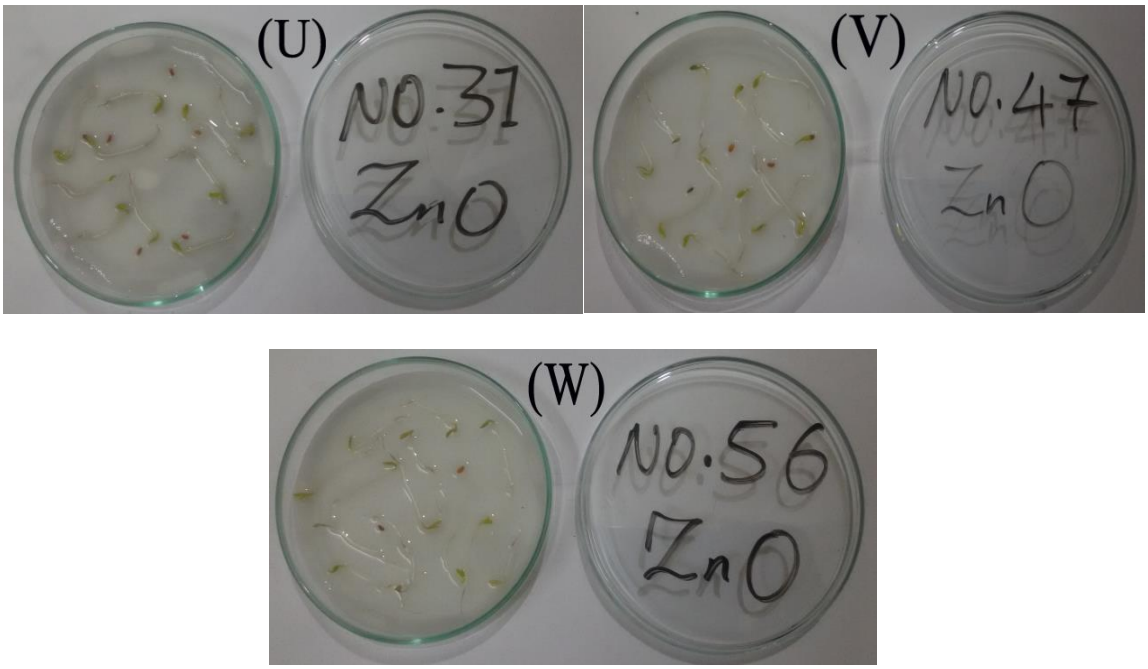

Figure S2. Root growth and seed germination percentage of *L. sativum* L. in FB1 solution during the HPO process; $[FB1]_0$ = 50 (mg/L), $[TiO_2]$ = 0.8 (g/L), ZnO = 1.2 (g/L), T = 25 ˚C and pH = 6.7.

Determination of mineralization rate constants

The plot of $ln(COD_0/COD)$, i.e., the dye solution initial and COD values (mg O_2/L) at a given time, versus time in Figure S3 represent straight lines for both UV-TiO_2 and UV-ZnO processes, from which the mineralization rate constants have been determined.

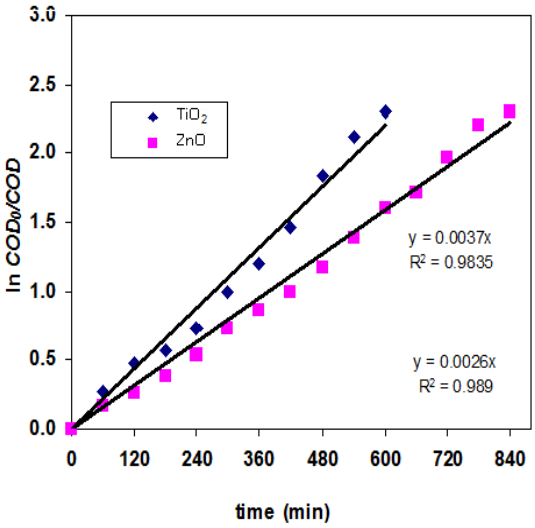

Figure S3. Pseudo-first-order kinetic rate constants for the photocatalytic mineralization of FB1 using TiO_2 and ZnO catalysts: $[FB1]_0$ = 50 (mg/L), $[TiO_2]$ = 0.8 (g/L), [ZnO] = 1.2 (g/L), T = 25 ˚C and pH = 6.7 (neutral).

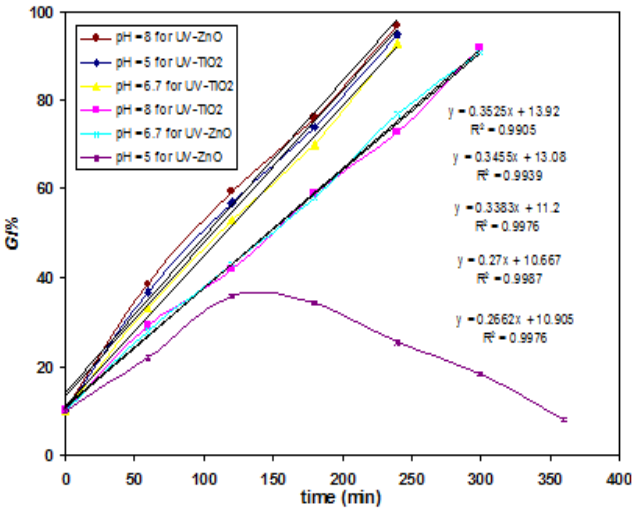

Figure S4. The variation of *GI*% versus time for detoxification of FB1 by UV-TiO_2 and UV-ZnO processes at different pH values: $[FB1]_0$ = 50 (mg/L), $[TiO_2]$ = 0.8 (g/L), [ZnO] = 1.2 (g/L) and T = 25 °C.

Determination of Langmuir-Hinshelwood kinetic rate constants

The plot of $1/k_{obs}$ versus $[FB1]_0$ represented in Figure S5 (A and B) shows a linear variation, confirming the Langmuir-Hinshelwood kinetic model for the initial rates of photocatalytic degradation [3]. Accordingly, the values of k_c and K_{LH} for each applied catalyst (TiO_2 and ZnO) have been calculated at different pH values (5, 6.7 and 8) from the intercept and slope of the straight lines.

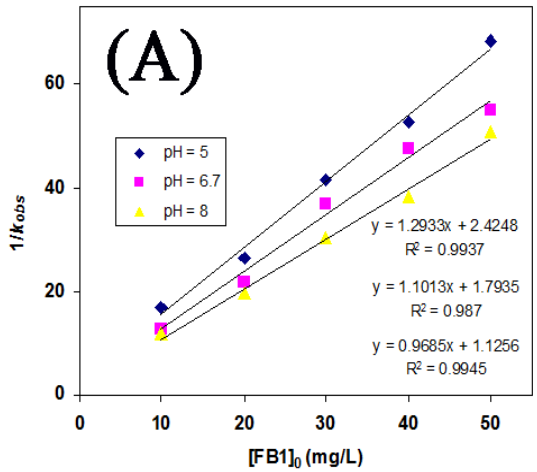

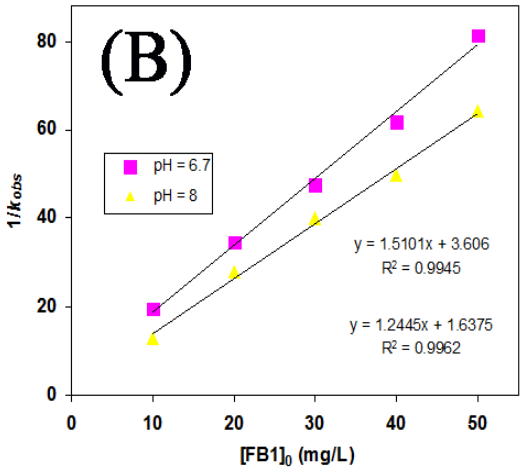

Figure S5. Variation of reciprocal of constant rate versus different initial concentrations of FB1 at different pH values (5, 6.7 and 8); [TiO_2] = 0.8 (g/L), [ZnO] = 1.2 (g/L) and T = 25 ˚C. (A): for UV-TiO_2 and (B): for UV-ZnO processes.

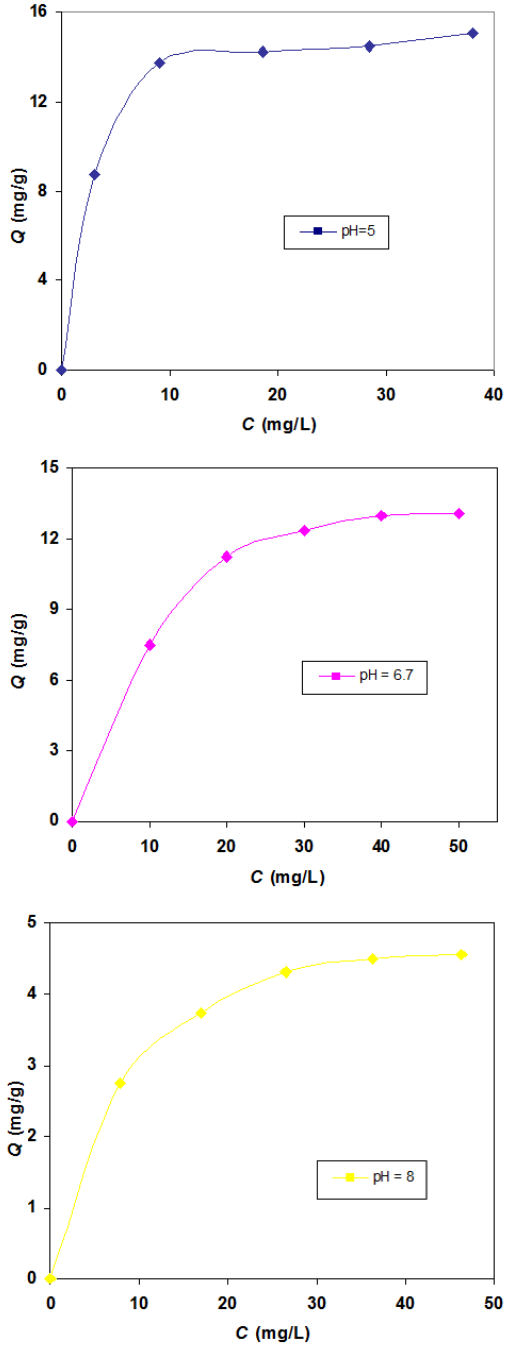

FigureS 6. Adsorption isotherm of FB1 on TiO_2 surface, quantity adsorbed (mg of adsorbed dye per gram of catalyst) as a function of equilibrium concentration: [TiO_2] = 0.8 (g/L), T = 25 ˚C.

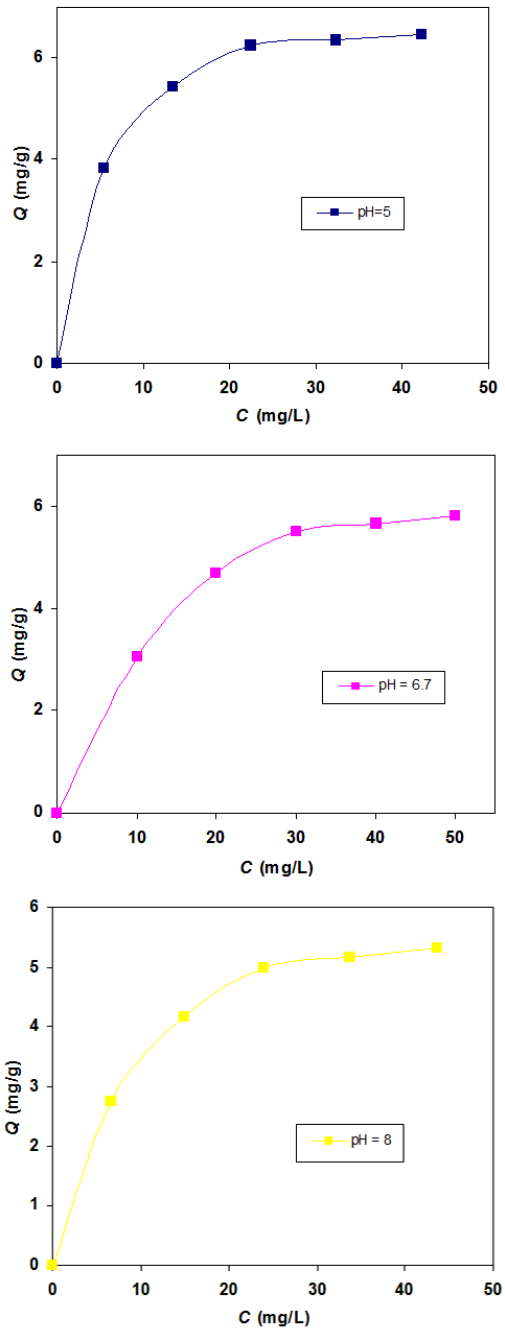

Figure S7. Adsorption isotherm of FB1 on the ZnO surface, and quantity adsorbed (mg of adsorbed dye per gram of catalyst) as a function of equilibrium concentration; [ZnO] = 1.2 (g/L), T = 25 ˚C.

Equilibrium dark adsorption

Based on previous studies, adsorption of pollution on catalyst surface would be described based on Langmuir model when the following assumptions were established: (i) sites of adsorption on the catalyst surface are limited, (ii) the surface of the catalyst could be covered only by one layer, (iii) etching available sites on the catalyst surface can adsorb just one molecule, (iv) the adsorption reaction is reversible, (v) the catalyst surface is homogeneous and (vi) there is no interaction between the adsorbed molecules [3]. To determine the Langmuir adsorption constant (K_{ads} in L/mg) and the maximum absorbable dye quantity (Q_{max} in mg/g), the C/Q versus C plot is provided in Figure S8 (A, B and C) for TiO_2 catalyst at pH values of 5, 6.7 and 8. Meanwhile, these constants were calculated for a ZnO catalyst using Figure S9 (A, B and C) at pH values of 5, 6.7 and 8.

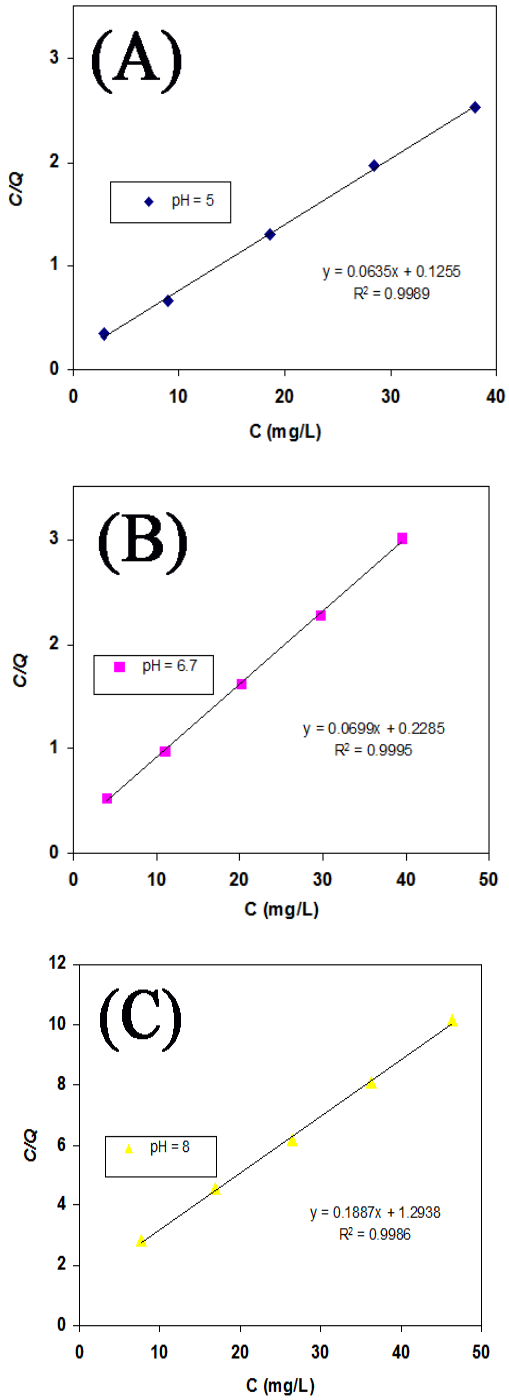

Figure S8. Establishment of Langmuir monolayer adsorption constants for adsorption of FB1 on TiO_2 catalyst at different pH values; [TiO_2] = 0.8 (g/L) and T = 25 °C. (A): pH of 5, (B): pH of 6.7 (neutral) and (C): pH of 8.

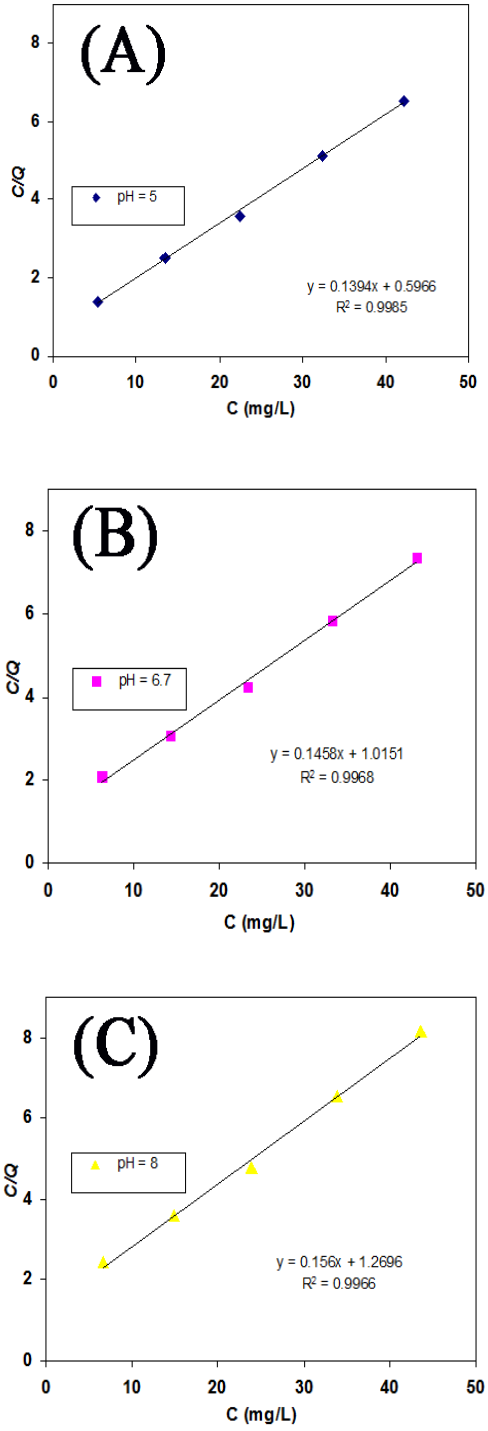

Figure S9. Establishment of Langmuir monolayer adsorption constants for adsorption of FB1 on ZnO catalyst at different pH values; [ZnO] = 1.2 (g/L) and T = 25 ˚C. (A): pH of 5, (B): pH of 6.7 (neutral) and (C): pH of 8.

Determination of effective concentration EC_{50}

The effect of different concentrations of FB1 (10, 20, 30, 40, and 50 mg/L) that induce inhibition of *L. sativum* L. root growth and seed germination percentage has been illustrated in Figure S10.

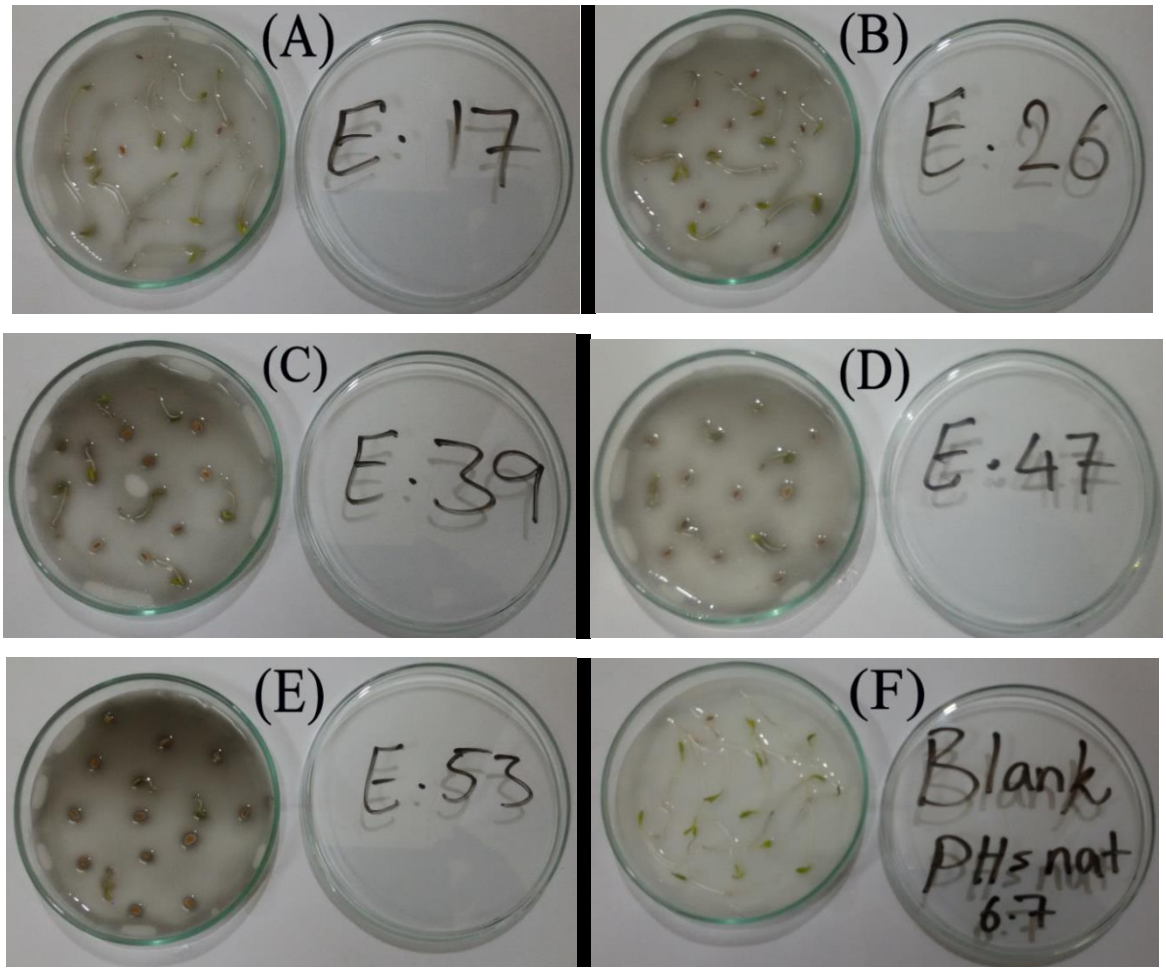

Figure S10. Evaluation of effective concentration (EC_{50}) for FB1; T = 25 °C and pH = 6.7 (neutral). (A): $[FB1]_0$ = 10 (mg/L), (B): $[FB1]_0$ = 20 (mg/L), (C): $[FB1]_0$ = 30 (mg/L), (D): $[FB1]_0$ = 40 (mg/L), (E): $[FB1]_0$ = 50 (mg/L) and (F): Control (distilled water).

Photocatalytic degradation kinetics

The initial concentration of the target pollutant has an important effect on the photocatalytic degradation rate. That is, the rate constant (k_{obs}) decreased with an increase in the initial concentration of the target dye. The photocatalytic degradation kinetics of FB1 aqueous solutions containing TiO_2 or ZnO catalysts have been described based on a well-known pseudo-first-order model. Accordingly, the values of k_{obs} were obtained in different initial concentrations and pH values, and the results are listed in Table S1.

Table S1. Pseudo-first-order rate constant values for the different initial concentrations of FB1 at various pH values: [TiO_2] = 0.8 (g/L), [ZnO] = 1.2 (g/L) and T = 25 °C.

	$[FB1]_0$ in (mg/L)	$k_{obs} \times 10^2$ (1/min) for TiO_2 in initial pH of			$k_{obs} \times 10^2$ (1/min) for ZnO in initial pH of		
		5	6.7	8	5	6.7	8
1	10	5.90	7.31	8.50	-	5.15	7.69
2	20	3.79	4.62	5.11	-	2.92	3.62
3	30	2.42	2.68	3.29	-	2.08	2.50
4	40	1.88	2.11	2.60	-	1.62	2.01
5	50	1.46	1.82	1.97	-	1.23	1.56

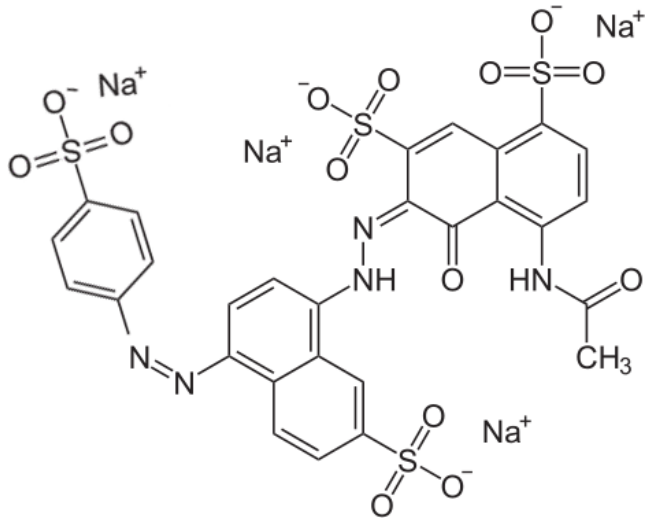

Figure S11. Chemical structure of Food Black 1 (FB1).

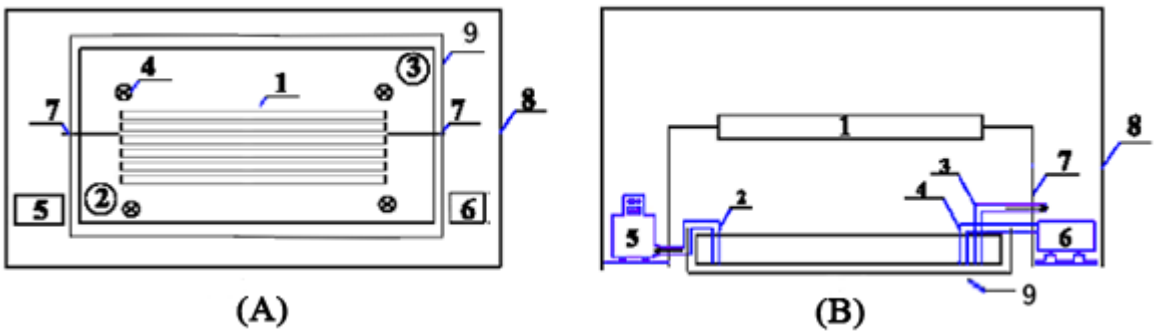

Figure S12. Schematic view of the photo-reactor: (A) top view, (B) front view. Photo-reactor parts: 1, UV lamps; 2, solution suction site; 3, solution return site; 4, air bubbling site; 5, circulating pump; 6, micro-air compressor; 7, lamp holder, 8; aluminum thin layer cover; 9, external jacket for regulation of temperature.

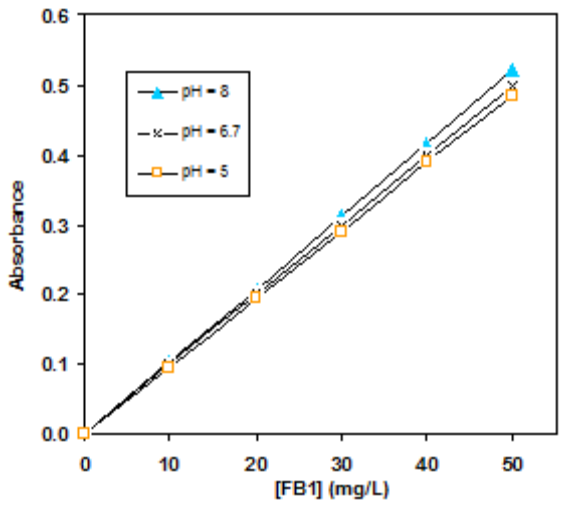

Figure S13. The calibration chart for measuring FB1 concentration at different pH values of 5, 6.7 and 8; T = 25 °C.

References cited in the Supplementary Information

[1] S.P. Kim, M.Y. Choi, H.C. Choi, Photocatalytic activity of SnO_2 nanoparticles in methylene blue degradation, Materials Research Bulletin 74 (2016) 85-89.

[2] D. Chebli, F. Fourcade, S. Brosillon, S. Nacef, A. Amrane, Supported photocatalysis as a pre-treatment prior to biological degradation for the removal of some dyes from aqueous solutions; Acid Red 183, Biebrich Scarlet, Methyl Red Sodium Salt, Orange II, Journal of Chemical Technology & Biotechnology 85 (2010) 555-563.

[3] S. Khezrianjoo, H.D. Revanasiddappa, Langmuir-Hinshelwood kinetic expression for the photocatalytic degradation of Metanil Yellow aqueous solutions by ZnO catalyst, Chemical Sciences Journal 2012 (2012) 1-7.